PNAS PLUS

IL-33/ST2 signaling excites sensory neurons and mediates itch response in a mouse model of poison ivy contact allergy

Boyi Liu[a,b,1], Yan Tai[b], Satyanarayana Achanta[b], Melanie M. Kaelberer[b], Ana I. Caceres[b], Xiaomei Shao[a], Jianqiao Fang[a], and Sven-Eric Jordt[b,1]

[a]Department of Neurobiology and Acupuncture Research, The Third Clinical Medical College, Zhejiang Chinese Medical University, Hangzhou, Zhejiang 310053, People's Republic of China; and [b]Department of Anesthesiology, Duke University School of Medicine, Durham, NC 27710

Edited by Diana M. Bautista, University of California, Berkeley, CA, and accepted by Editorial Board Member David E. Clapham October 14, 2016 (received for review April 27, 2016)

Poison ivy-induced allergic contact dermatitis (ACD) is the most common environmental allergic condition in the United States. Case numbers of poison ivy ACD are increasing due to growing biomass and geographical expansion of poison ivy and increasing content of the allergen, urushiol, likely attributable to rising atmospheric CO_2. Severe and treatment-resistant itch is the major complaint of affected patients. However, because of limited clinical data and poorly characterized models, the pruritic mechanisms in poison ivy ACD remain unknown. Here, we aim to identify the mechanisms of itch in a mouse model of poison ivy ACD by transcriptomics, neuronal imaging, and behavioral analysis. Using transcriptome microarray analysis, we identified IL-33 as a key cytokine up-regulated in the inflamed skin of urushiol-challenged mice. We further found that the IL-33 receptor, ST2, is expressed in small to medium-sized dorsal root ganglion (DRG) neurons, including neurons that innervate the skin. IL-33 induces Ca^{2+} influx into a subset of DRG neurons through neuronal ST2. Neutralizing antibodies against IL-33 or ST2 reduced scratching behavior and skin inflammation in urushiol-challenged mice. Injection of IL-33 into urushiol-challenged skin rapidly exacerbated itch-related scratching via ST2, in a histamine-independent manner. Targeted silencing of neuronal ST2 expression by intrathecal ST2 siRNA delivery significantly attenuated pruritic responses caused by urushiol-induced ACD. These results indicate that IL-33/ST2 signaling is functionally present in primary sensory neurons and contributes to pruritus in poison ivy ACD. Blocking IL-33/ST2 signaling may represent a therapeutic approach to ameliorate itch and skin inflammation related to poison ivy ACD.

itch | pain | cytokine | IL-33 | allergic contact dermatitis

Allergic contact dermatitis (ACD) is a common allergic skin condition caused by environmental or occupational allergens (1). In the United States, the most common cause of ACD is contact with poison ivy, which affects >10 million Americans per year (2, 3). Poison ivy ACD is also a serious occupational hazard, particularly among firefighters, forestry workers, and farmers, accounting for 10% of total U.S. Forest Services lost-time injuries, and it often torments outdoor enthusiasts as well (3, 4). The major allergen in poison ivy is urushiol, contained in the oleoresinous sap of the plant and of related plants (e.g., poison oak and poison sumac) (5). An estimated 50–75% of Americans are sensitized to urushiol (6). Elevated atmospheric carbon dioxide and warming temperatures have increased the biomass of poison ivy and related plants, widened their geographic distribution, and increased plant urushiol content (7). These factors will likely increase allergenicity and result in even larger case numbers of poison ivy ACD in the future (8).

The clinical manifestations of poison ivy-induced ACD are intense and persistent itch (pruritus), burning sensation, skin rashes, and swelling, followed by the appearance of vesicles in severe cases (2, 3, 9). Skin inflammation and pruritus last for weeks. The severe itch usually triggers scratching that is hard to control, especially among children, and further injures the skin (10). Scratching exacerbates the inflammation and stimulates nerve fibers, leading to even more itch and scratching. This itch–scratch cycle can cause skin infections that require antibiotic treatment. Antihistamines are usually ineffective for treating pruritus associated with poison ivy ACD, although they are still commonly used (2, 11). Patients with severe symptoms are treated with high-dose corticosteroid regimens, which frequently have side effects and are effective only if administered shortly after exposure.

The pruritic mechanisms in poison ivy ACD remain largely unknown because of very limited clinical data and poorly characterized animal models. Itch signals are generated by a subset of primary afferent sensory neurons that innervate the skin (12). Recent studies using rodent models of pruritic conditions identified a range of non-histaminergic endogenous itch mediators acting on sensory neurons and neuronal receptor systems signaling itch. These include cytokines such as IL-31, CXCL-10, or TSLP (thymic stromal lymphopoietin); transmitters such as serotonin; and their cognate receptors and coupled ion channels (13–15). These studies used either chemicals eliciting acute itch (such as chloroquine) or ACD rodent models induced by synthetic allergens not present in the environment [2,4-dinitrofluorobenzene (DNFB) oxazolone, and others] (14, 16–18).

We contributed to these efforts, identifying the ion channel TRPA1 (transient receptor potential ankyrin 1) as a key target to

Significance

In the United States, the most common cause of allergic contact dermatitis (ACD) is contact with poison ivy. Severe itch and skin inflammation are the major manifestations of poison ivy-induced ACD. In this study, we have established a critical role of IL-33/ST2 (interleukin 33/growth stimulation expressed gene 2) signaling in both itch and skin inflammation of poison ivy-induced ACD and revealed a previously unidentified interaction of IL-33/ST2 signaling with primary sensory neurons that may underlie the pruritic mechanisms of poison ivy-induced ACD. Blocking IL-33/ST2 signaling may represent a therapeutic approach to ameliorate itch and skin inflammation related to poison ivy dermatitis and, possibly, other chronic itch conditions in which IL-33/ST2 signaling may participate.

Author contributions: B.L. and S.-E.J. designed research; B.L., Y.T., and A.I.C. performed research; M.M.K., X.S., and J.F. contributed new reagents/analytical tools; B.L., Y.T., S.A., and A.I.C. analyzed data; and B.L. and S.-E.J. wrote the paper.

The authors declare no conflict of interest.

This article is a PNAS Direct Submission. D.M.B. is a Guest Editor invited by the Editorial Board.

[1]To whom correspondence may be addressed. Email: sven.jordt@duke.edu or boyi.liu@foxmail.com.

This article contains supporting information online at www.pnas.org/lookup/suppl/doi:10.1073/pnas.1606608113/-/DCSupplemental.

suppress itch in a mouse ACD model induced by the synthetic allergen oxazolone (16). To examine whether these pathways also contribute to itch in poison ivy ACD, we established a mouse model induced by cutaneous sensitization and challenge with urushiol. This model mimics many key clinical features of poison ivy-induced ACD, including skin inflammation and severe itch (16). TRPA1 inhibition was less efficacious in this model, suggesting that poison ivy ACD engages as-yet-unknown inflammatory and pruritic pathways (16).

The aim of the present study is to reveal these pathways through an unbiased approach by using transcriptome microarray analysis of urushiol-induced genes in the mouse skin, validation by quantitative PCR (qPCR) and biochemistry, neuronal functional imaging, and pharmacological and behavioral testing.

Results

Urushiol-Induced ACD Triggers the Release of IL-33 from the Inflamed Skin. To search for potential endogenous pruritogens involved in the pruritus caused by urushiol-induced ACD, we carried out a mouse transcriptome microarray analysis to study gene expression profiles of the skin isolated from urushiol-challenged and unchallenged (acetone-treated) mice. For comparison, we included the well-established oxazolone-induced ACD mouse model. Mice were sensitized with 2.0% (wt/vol) oxazolone or urushiol on the abdominal skin, followed by challenges on the nape of neck 5 d later with 0.5% oxazolone or urushiol, a concentration known to elicit ACD in sensitized humans (Fig. 1*A*) (19). We found that, during the third and fifth urushiol challenge, mice usually developed a stable dermatitis condition and long-lasting scratching toward the neck. Therefore, mouse neck skin samples were collected after the fifth challenge. Total RNA from neck skins of unchallenged mice and from the mice that had received urushiol or oxazolone treatment were analyzed by using hybridization with a mouse transcriptome microarray. A total of 3,612 genes, which represents 5.5% of total genes (65,956), was identified to be significantly up- or down-regulated (greater than twofold; $P < 0.05$) in mouse skin upon urushiol treatment (Tables S1 and S2). Among these differentially regulated genes, we were especially interested in inflammatory cytokines and chemokines that are abundantly up-regulated. Fig. 1*B* illustrates the top 15 inflammatory cytokines and chemokines that are significantly up-regulated. Among these genes, some well-established inflammatory markers, such as IL-1β and CXCL-2, were highly up-regulated in both the oxazolone and urushiol groups. Of particular interest was cytokine IL-33, which was significantly up-regulated in both oxazolone- and urushiol-treated groups. IL-33 has not previously been implicated in itch, but neutralizing antibodies against IL-33 were shown to attenuate skin swelling in a mouse ACD model and in humans (20, 21). IL-33 expression is also enhanced in human ACD skin (21). More importantly, skin-specific expression of IL-33 can elicit atopic dermatitis-like inflammation and scratching behavior in mice (22). In the present study, we therefore investigated the possible involvement of this cytokine in itch caused by poison ivy ACD.

qPCR analysis confirmed that IL-33 transcription was significantly up-regulated in both oxazolone- and urushiol-treated groups compared with acetone (Fig. 1*C*). ELISA confirmed a corresponding increase in IL-33 protein levels in the inflamed skin, but not in plasma (Fig. 1 *D* and *E*). Finally, increased levels of IL-33 were detected in mouse skin sections from both oxazolone- and urushiol-treated groups by immunofluorescence staining (Fig. 1 *F* and *G*). Immunofluorescence further revealed that IL-33 was extensively expressed in cells localized in the epidermis of skin (Fig. 1*F*). Double immunofluorescence staining showed that IL-33–positive cells closely overlap with cells stained with keratin 14, a specific marker for keratinocytes (Fig. 1*H*). We conclude that IL-33 is significantly increased in the inflamed skin in urushiol-induced ACD mice because of increased production and release from keratinocytes.

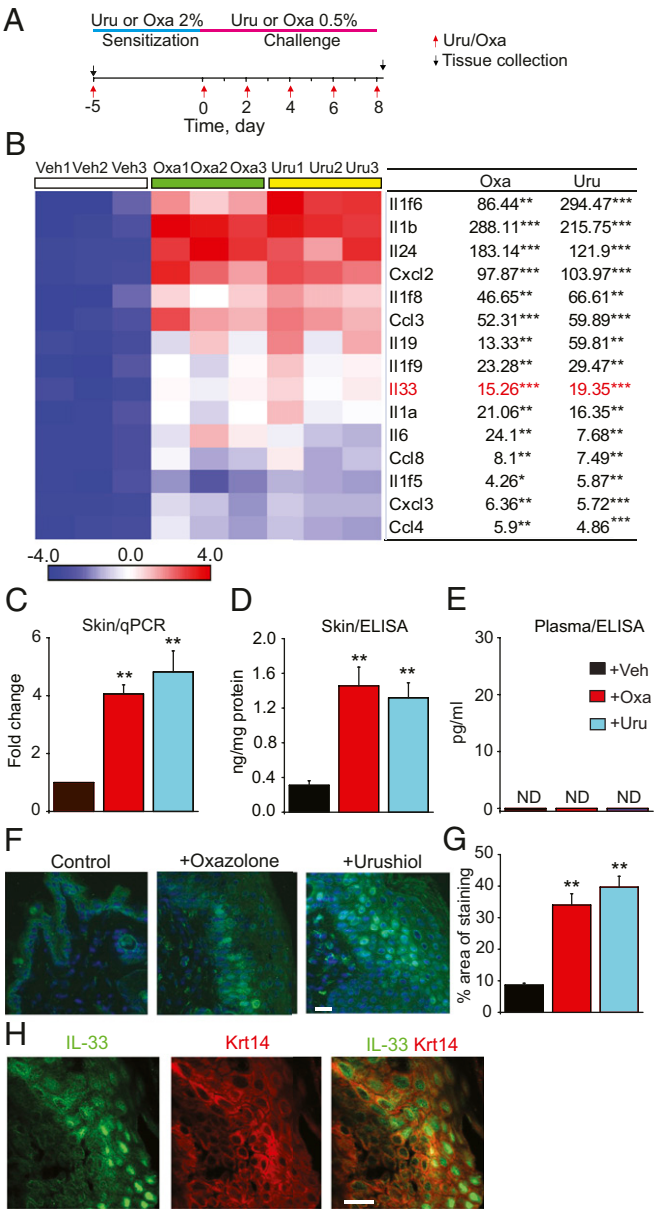

Fig. 1. Mouse transcriptome microarray analysis of oxazolone- or urushiol-challenged mouse skin. (*A*) Scheme of treatment in urushiol- or oxazolone-induced mouse ACD model. (*B*) Heat map showing top 15 most up-regulated inflammatory cytokines and chemokines in oxazolone (Oxa)- and urushiol (Uru)-challenged mouse neck skin, identified by mouse transcriptome microarray analysis. Vehicle group (Veh) mice were treated with acetone. $n = 3$ mice per group. (*C*) Fold changes of IL-33 gene transcript in skin samples from oxazolone- and urushiol-challenged mouse by qPCR. (*D* and *E*) IL-33 from skin and plasma of mice by ELISA. $n = 7$ or 8 mice per group. ND, not detectable. (*F*) Immunofluorescence images of IL-33 staining (green) in mouse neck skin from frozen sections. Nuclei were labeled with DAPI (blue). (*G*) Summary of IL-33 immunostaining in *F*. $n = 7$ or 8 mice per group. (*H*) Double immunostaining showing the overlapping of IL-33 with keratin 14 in the skin of urushiol-induced ACD mice. $^*P < 0.05$; $^{**}P < 0.01$; $^{***}P < 0.001$ vs. vehicle/control group. One-way ANOVA followed by Tukey post hoc test was used for statistical analysis. (Scale bars, 20 μm.)

IL-33–Specific Receptor ST2 Is Expressed in Peripheral Sensory Neurons. Although numerous studies have shown that IL-33 acts on immune cells, IL-33 signaling in peripheral sensory neurons has not been reported. IL-33 signals through the IL-33 receptor complex, a heterodimer consisting of the accessory chain IL-1 receptor-like 1 (IL-1RAcP) and a membrane-bound IL-33–specific ST2 chain (23).

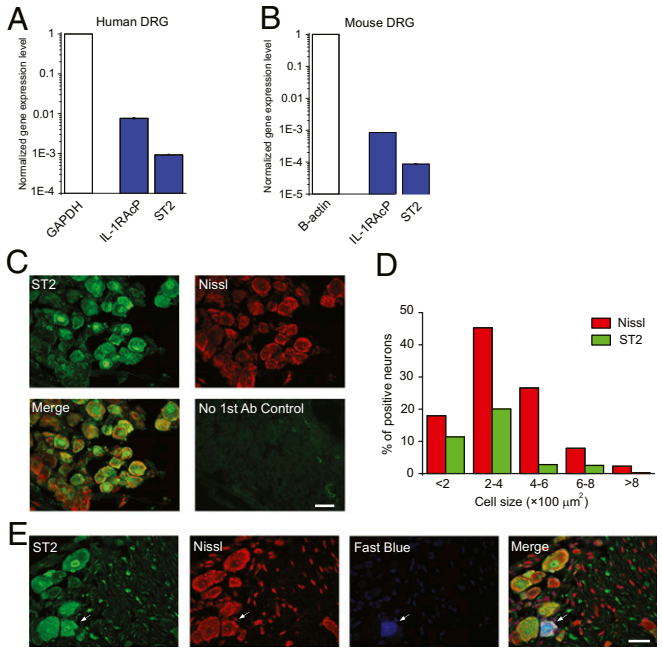

Fig. 2. Analysis of IL-33 receptor ST2 expression in DRG neurons. (*A* and *B*) Summary of gene expression levels of IL-33 receptor complex IL-1RAcP and ST2 in human (*A*) and mouse (*B*) DRGs. Mouse β-actin and human GAPDH were used as housekeeping genes. (*C*) Immunostaining showing the immunoreactivity of IL-33 receptor ST2 (green) in mouse cervical DRG neurons (identified by Nissl staining; red). (Magnification: 60×.) (*D*) Cell size distribution frequency of ST2-positive and Nissl staining-positive neurons (636 neurons/12 inconsecutive sections/5 mice). (*E*) ST2 is expressed in cutaneous Fast Blue (purple) labeled DRG neurons indicated by white arrows. (Scale bars, 20 μm.)

We detected both ST2 and IL-1RAcP transcripts in human and mouse dorsal root ganglia (DRGs) by using qPCR (Fig. 2 *A* and *B*). Immunofluorescence staining further showed that ST2 was expressed by 34.3% of DRG neurons of mouse (218 of 636 neurons), mainly in small and medium-sized neurons (Fig. 2 *C* and *D*). The specificity of ST2 antibody was confirmed by negative control staining without first antibody (Fig. 2*C*), and staining with first antibody preabsorbed with a blocking peptide with the ST2-derived antigenic sequence (Fig. S1 *A* and *B*).

Itch is mediated by a subset of peripheral cutaneous sensory neurons (12). To study the expression of ST2 in the cutaneous sensory neurons, we used retrograde labeling dye Fast Blue to specifically label skin-innervating DRG neurons. This approach revealed that ST2 is expressed in skin-innervating DRG neurons, with 8.3% of ST2-expressing neurons labeled with Fast Blue (Fig. 2*E*, white arrow). Immunofluorescence analysis identified ST2 costaining with IL-1RAcP and TRPV1, but not with GS, a marker for satellite glial cells (Fig. S2*A*). A total of 21.5% of ST2 immunoreactive neurons showed IL-1RAcP staining and 57.1% showed TRPV1 costaining. We also identified costaining of ST2 with PGP9.5-positive free nerve endings in skin sections (Fig. S2*B*).

IL-33 Produces Ca^{2+} Responses in DRG Neurons Through Its Receptor ST2. We proceeded to explore whether ST2 receptors are functional in DRG neurons by testing the effects of IL-33 on intracellular Ca^{2+} mobilization of cultured cervical DRG neurons (C1-T1). In our initial experiments, we observed that IL-33 produced Ca^{2+} responses in neurons dissociated from both control and urushiol-challenged mice, with larger numbers of neurons responding in the latter amounting to 12.0 ± 1.3% of total KCl-responsive (KCl^+) neurons (Fig. 3 *A*–*D*). Chloroquine (CQ), a well-established pruritogen that causes itch via MrgA3 in DRG neurons (17), was applied after IL-33 to determine whether these populations overlap. Representative patterns of Ca^{2+} responses of these neurons are shown in Fig. 3*B*. Venn diagram analysis revealed that 51.9% of IL-33–responsive neurons also responded to CQ (Fig. 3*C*). In addition, 75.0% of IL-33–responsive neurons also responded to histamine (Fig. 3*C*). We found that 67.6% and 85.3% of IL-33–responsive neurons are activated by mustard oil (MO) and capsaicin (Cap), respectively (Fig. 3 *B* and *C*). In summary, Ca^{2+} imaging revealed that IL-33 induces robust Ca^{2+} responses in a subset of DRG neurons that also mediate pain and/or itch responses.

Removal of extracellular Ca^{2+} or addition of the broad spectrum TRP channel blocker ruthenium red almost totally abolished

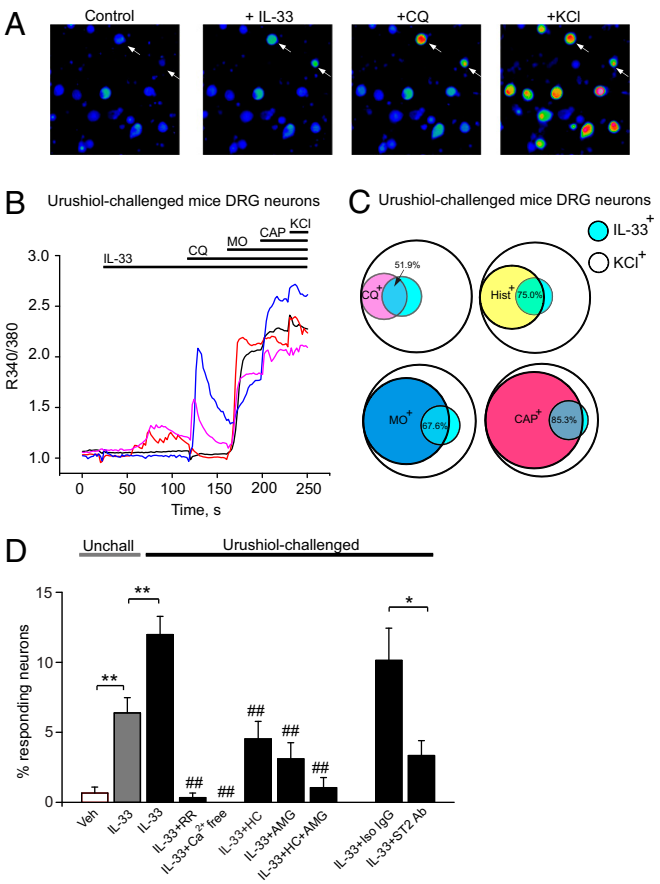

Fig. 3. IL-33 induces Ca^{2+} mobilization in cultured DRG neurons isolated from urushiol-challenged mice. (*A*) Pseudocolor Fura-2 ratiometric images of DRG neurons isolated from C1-T1 DRGs of mice challenged with urushiol. Images show Ca^{2+} responses of DRG neurons in control condition and upon IL-33 (1 μg/mL), CQ (300 μM), and KCl (40 mM) application. White arrows indicate neurons that responded positively to IL- 33. (Magnification: 10×.) (*B*) Time course traces illustrate the different types of Ca^{2+} responses upon IL-33 and CQ application: cell responding to both IL-33 and CQ, pink; cell responding to IL-33 only, red; cell responding to CQ only, blue; cell responding to neither IL-33 nor CQ, black. (*C*) Venn diagram showing the overlapping of IL-33–positive ($IL\text{-}33^+$) with CQ-positive, histamine (Hist)-positive, mustard oil (MO)-positive, and capsaicin (Cap)-positive neuronal populations. Each Venn diagram contains 200–300 DRG neurons. A neuron was considered $IL\text{-}33^+$ if the peak Ca^{2+} response was >20% of baseline. (*D*) Summary of percentages of DRG neurons responding to vehicle (Veh; 0.1% BSA) and IL-33 in control, Ca^{2+}-free extracellular solution, ruthenium red (RR; 10 μM), HC-030031 (HC; 100 μM), AMG9810 (AMG; 6 μM), isotype control IgG (Iso IgG; 0.5 mg/mL), and ST2-neutralizing antibody (0.5 mg/mL)-treated conditions. A total of 6–12 fields of observation were included in each group (each group contains 300–800 neurons from three to five mice). $^*P < 0.05$; $^{**}P < 0.01$; $^{\#\#}P < 0.01$ compared to IL-33, urushiol-challenged. Student's *t* test or one-way ANOVA followed by Tukey post hoc test was used for statistical analysis.

the percentage of IL-33–responsive neurons, suggesting that TRP ion channels may be acting downstream of IL-33 pathways (Fig. 3*D*). A TRPA1-specific blocker, HC-030031, and a TRPV1-specific blocker, AMG9810, both significantly reduced IL-33 responses (Fig. 3*D*). Coadministration of HC-030031 and AMG9810 further reduced the percentage of IL-33–responsive neurons (Fig. 3*D*). Pretreating neurons with a ST2-specific monoclonal neutralizing antibody also significantly reduced the percentage of IL-33–responsive neurons (Fig. 3*D*). Together, these results demonstrate that the IL-33–induced Ca^{2+} response in DRG neurons is largely mediated by TRP-like channels, possibly TRPA1 and TRPV1, downstream of neuronal ST2 receptors.

IL-33/ST2 Signaling Mediates Chronic Scratching Behavior and Skin Inflammation in Urushiol-Challenged Mice. To determine whether IL-33 was involved in the chronic scratching behavior associated with urushiol-induced ACD, we examined the effects of an IL-33–neutralizing antibody on scratching behavior of mice after the third urushiol challenge. Urushiol-challenged mice were administered i.p. either the IL-33–neutralizing antibody (15 μg per mouse, i.p.) or an isotype control IgG (goat IgG = Iso IgG(1), 15 μg per mouse, i.p.) daily, starting from day 0 until day 4 (Fig. 4*A*). Unchallenged mice (acetone-treated) received isotype control IgGs (i.p.) only. IL-33–neutralizing antibody significantly reduced the scratching behavior of mice at the 0-, 4-, and 24-h time points (Fig. 4*B*). We continued to examine whether ST2 was also involved in the scratching behaviors of mice in urushiol-induced ACD. ST2-neutralizing antibody (50 μg per mouse, i.p.) or isotype control IgG (rat IgG = Iso IgG(2), 50 μg per mouse, i.p.) were administered i.p. to urushiol-challenged mice in a similar treatment regimen (Fig. 4*A*). ST2-neutralizing antibody significantly reduced the scratching behavior of mice at the 0-, 4-, and 24-h time points (Fig. 4*C*). In addition, IL-33– and ST2-neutralizing antibodies did not affect motor coordination behavior in the mouse rotarod assay (Fig. 4*D*).

We proceeded to examine the effects of IL-33– and ST2-neutralizing antibody treatment on skin inflammation. Consistent with our previous observation (16), sensitization and challenge of the mouse neck skin with urushiol produced a strong increase in skin bifold thickness, transepidermal water loss (TEWL), and dermatitis score (Fig. S3). Daily treatment with IL-33– or ST2-neutralizing antibodies produced a modest, although significant, reduction in skin bifold thickness (Fig. S3 *A* and *B*). In addition, antibody treatment significantly reduced the TEWL and dermatitis score associated with ACD (Fig. S3 *C* and *D*). Collectively, these findings support the hypothesis that IL-33/ST2 signaling is involved in chronic scratching behavior and skin inflammation of urushiol-induced mouse ACD.

Exogenous IL-33 Exacerbates Itch-Related Scratching Behaviors and Skin Inflammation in Urushiol-Induced ACD Mice. To gain further insights into the role of IL-33 in chronic itch, we examined the potential behavioral effects of IL-33 in urushiol-induced mouse ACD. Right after the third urushiol challenge of the neck skin, a single dose of IL-33 [300 ng per site, intradermally (i.d.)] or PBS was injected into the nape of the neck (Fig. 5*A*). As expected, urushiol-challenged mice showed scratching behavior compared with acetone-treated controls (Fig. 5 *B* and *C*). Notably, we observed that IL-33 injection robustly enhanced the scratching behaviors in the urushiol-challenged mice at both the 0- and 4-h time points (Fig. 5 *B*–*D*). Two-way ANOVA analysis indicated significant differences between the IL-33– and vehicle-injected groups (Fig. 5 *B* and *C*). IL-33 began to take effect within 5 min after the injection, indicating a rapid action of IL-33 in eliciting scratching behavior in urushiol-challenged mice (Fig. 5*B*). In contrast, IL-33 injection into naïve mice did not elicit significant scratching during the first 30 min (Fig. 5*D*). These data indicate that IL-33 is more potent in inducing scratching behaviors in mice with fully established urushiol ACD.

We continued by determining whether the potentiating effect of IL-33 on scratching behavior in urushiol-induced ACD mice is mediated through the ST2 receptor. IL-33 together with ST2-neutralizing antibody or isotype control IgG were coinjected s.c. into the neck skin of urushiol-induced ACD mice. The ST2-neutralizing antibody almost completely abolished the potentiating effect of IL-33 on scratching at both the 0- and 4-h time points (Fig. 5*E*). Thus, we have established a pivotal role of

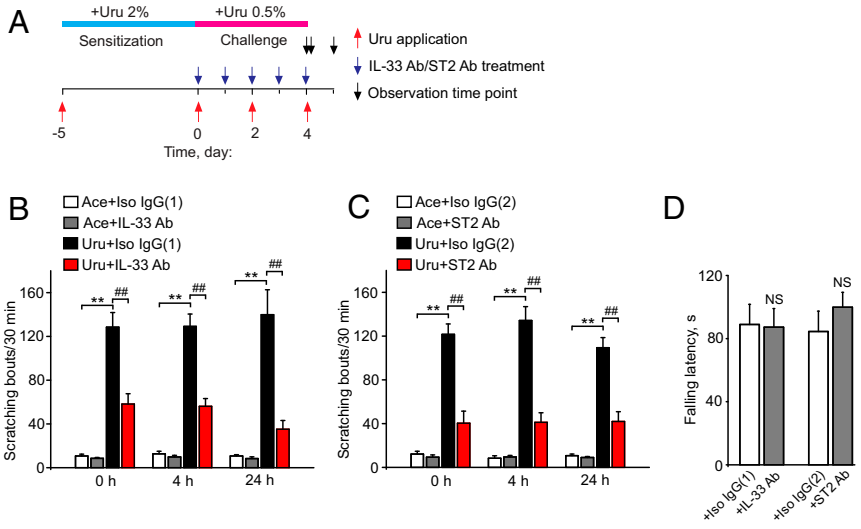

Fig. 4. Effects of inhibition of IL-33/ST2 signaling on chronic itch in urushiol-challenged mice. (*A*) Treatment of urushiol-induced mouse ACD model. Mice were treated (i.p.) with isotype control IgGs (Iso IgGs) or IL-33– or ST2-neutralizing antibody (Ab) every day for a total of five times. Scratching behaviors were monitored at 0-, 4-, and 24-h time points as indicated. (*B* and *C*) Summarized scratching behaviors of unchallenged mice (Ace) and urushiol-challenged mice (Uru) after the treatment with isotype control IgGs, IL-33–neutralizing (15 μg per mouse), or ST2-neutralizing (50 μg per mouse) antibody. (*D*) Motor coordination behavior measured by rotarod. Mice were treated with isotype control IgGs or IL-33, ST2 antibody. $n = 7$ or 8 mice per group. $^{**}P < 0.01$; $^{\#\#}P < 0.01$; NS, no significance. One-way ANOVA followed by Tukey post hoc test or Student's *t* test was used for statistical analysis.

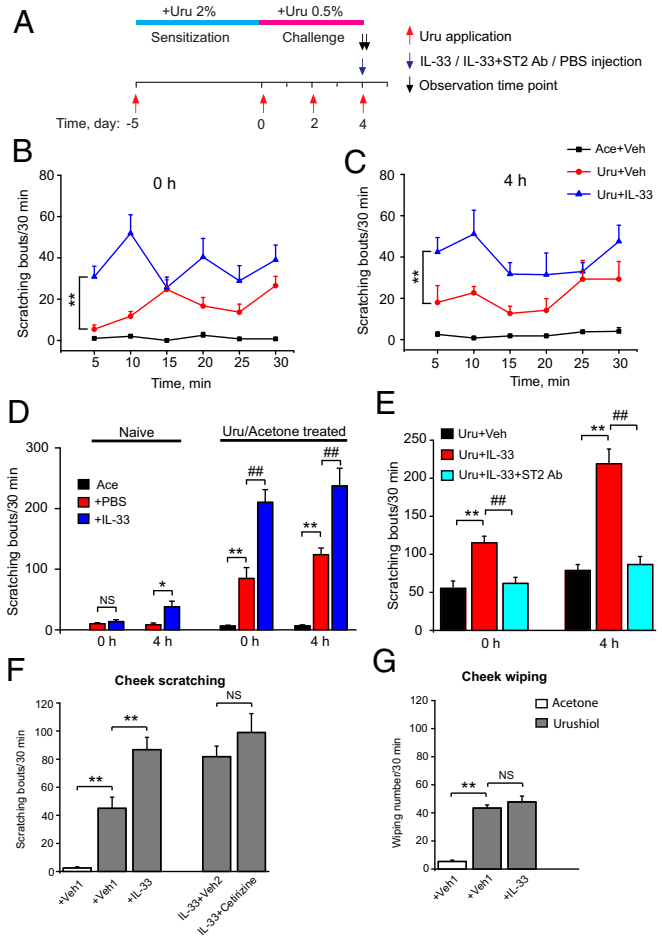

Fig. 5. IL-33 promotes itch-related scratching in urushiol-induced ACD mice through ST2. (*A*) Experimental scheme of urushiol-induced ACD on mouse neck. (*B* and *C*) Scratching behavior at 0 h (*B*) and 4 h (*C*) in unchallenged (acetone-treated; Ace) and urushiol-challenged (Uru) mice in 5-min intervals during a 30-min period after vehicle (0.1% BSA) or IL-33 (+IL-33; 300 ng per site) injection at the nape of the neck. (*D*) Summarized scratching behavior at 0- and 4-h time point for the entire 30-min recording period. (*E*) Scratching behaviors of urushiol-challenged mice upon vehicle (0.1% BSA), IL-33–neutralizing (300 ng per site), and IL-33+ST2–neutralizing antibody (ST2 Ab; 50 μg per site) injection at the nape of neck at 0- and 4-h time points. (*F*) Effects of IL-33 or IL-33/cetirizine coadministration on cheek-scratching behavior recorded within 30 min after the third urushiol challenge of the cheek. Acetone group was challenged with acetone only. Cetirizine (10 mg/kg) or PBS was administered (i.p.) 30 min before IL-33 injection. Vehicle 1, 0.1% BSA in PBS (Veh1); Vehicle2, PBS (Veh2). (*G*) Cheek-wiping behavior in the same first three groups of mice shown in *F*. $n = 7$ or 8 mice per group. $^{*}P < 0.05$, $^{**}P < 0.01$, $^{\#\#}P < 0.01$. NS, no significance. One- or two-way ANOVA followed by Tukey post hoc test was used for statistical analysis.

IL-33 in mediating the chronic scratching in urushiol-induced ACD mouse.

Behavioral responses to itch and pain are difficult to distinguish. We therefore used a recently introduced rodent model in which pruritogenic (or algogenic) stimuli are applied to the cheek (24). After the third urushiol challenge on the cheek, urushiol-challenged mice showed more cheek-directed scratching and wiping behavior than acetone-treated mice (Fig. 5 *F* and *G*). Injection of IL-33 into the cheek of urushiol-challenged mice significantly increased scratching, but not wiping, compared with vehicle-injected mice (Fig. 5 *F* and *G*). The histamine H_1 receptor antagonist, cetirizine, had no effect on IL-33–induced cheek-scratching behavior (Fig. 5*F*). These results demonstrate that IL-33 can evoke itch-related behavior in the inflamed skin of urushiol-induced ACD mice via a histamine-independent mechanism.

DRG-Expressed ST2 Is Essential for the Itch Response of Urushiol-Induced ACD Mice. To examine the contribution of neuronal ST2 to the itch response of urushiol-induced ACD mouse, we intrathecally (i.t.) administered ST2-targeted siRNA to knock down its neuronal expression. Scrambled control siRNA was used as a control (Fig. 6*A*). qPCR confirmed that repeated i.t. delivery of ST2 siRNA significantly reduced *St2* gene expression in DRG neurons, without altering Il1rl2 or Il31ra gene expression (Fig. 6*B*). Spinal cord St2 gene expression was not significantly changed by siRNA treatment (Fig. 6*C*). ST2 protein expression in DRG neurons was also significantly reduced by siRNA treatment (Fig. 6 *D* and *E*). Notably, i.t. ST2 siRNA significantly attenuated the itch response and skin inflammation of urushiol-induced ACD mice, without altering locomotion activity of the mice (Fig. 6 *F*–*H*). Therefore, these results established a crucial role of ST2 expressed in DRG neurons in mediating the itch response of urushiol-induced ACD mice.

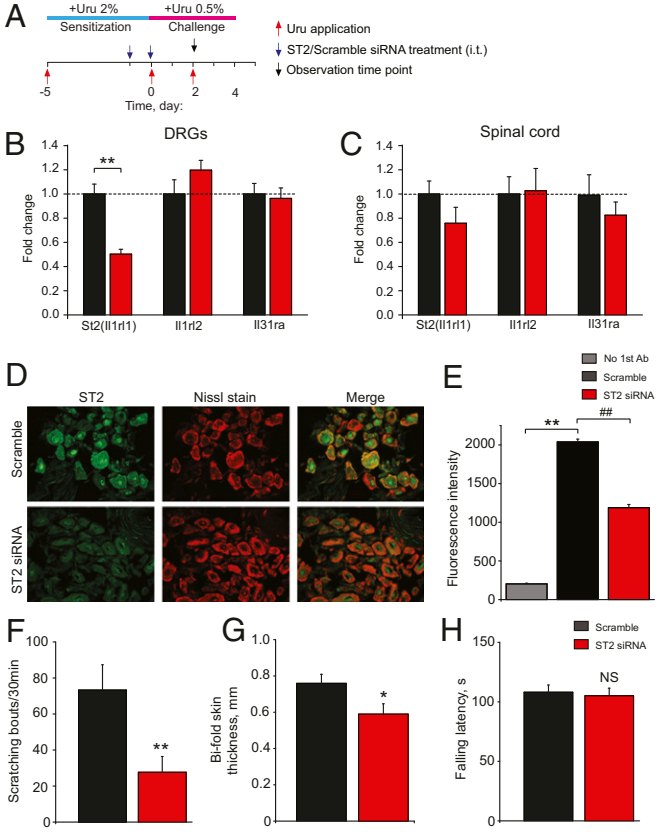

Fig. 6. Effects of DRG-specific knockdown of ST2 on the itch response of urushiol-induced ACD mice. (*A*) Protocol for i.t. delivery of ST2 siRNA or scrambled control siRNA to mice. (*B* and *C*) qPCR analysis of transcript levels of *St2* (*Il1rl1*), *Il1rl2*, and *Il31ra* in DRGs (*B*) or spinal cords (*C*) of ST2 siRNA or scrambled siRNA treatment groups. (*D*) Immunostaining of DRG sections showing analyzing expression of ST2 protein of ST2 siRNA- or scrambled siRNA-treated group. (Magnification: 60×.) (*E*) Summary of ST2 staining fluorescence intensities of neurons from ST2 siRNA or scrambled siRNA-treated mice. A total of 100–120 neurons pooled from five mice from each group were compared. (*F*) Analysis of scratching behavior of urushiol-induced ACD mice after i.t. injection of ST2 siRNA. (*G*) Bifold skin thickness of urushiol-induced ACD mice treated with ST2 siRNA or scrambled siRNA. (*H*) Comparison of motor coordination activity of siRNA-treated mice tested with rotarod. $n = 6$ or 7 mice per group. $^{*}P < 0.05$; $^{**}P < 0.01$; $^{\#\#}P < 0.01$. NS, no significance. Student's *t* test or one-way ANOVA followed by Tukey post hoc test was used for statistical analysis.

Discussion

Environmental exposure to poison ivy is the most common cause of ACD in the United States, representing a significant public health burden. ACD is elicited by direct contact with the plant or indirectly by contact with contaminated clothing, shoes, and tools. Inhalation of smoke from burning plant material is especially hazardous and can trigger severe respiratory allergic responses (2, 5). Strong and persistent itch and skin inflammation are the major manifestations of poison ivy ACD. In contrast to other environmental allergic conditions, little is known about the specific mechanisms underlying itch and skin inflammation in poison ivy-induced ACD.

Studies modeling ACD almost exclusively used synthetic experimental allergens, such as oxazolone and DNFB, that are not present in the environment. However, different allergens cause widely divergent immune responses, making it difficult to predict mechanisms and therapeutic strategies for ACD elicited by common environmental allergens such as urushiol (25, 26). We therefore optimized and characterized a mouse model of poison ivy ACD and applied transcriptomic, biochemical, neurophysiological, and behavioral methods to identify the inflammatory and pruritic mechanisms engaged in murine poison ivy ACD. We identified a critical role of IL-33/ST2 signaling in both itch and skin inflammation in this model and revealed a previously unknown interaction of IL-33 with primary sensory neurons that may underlie the itch mechanism of urushiol-induced ACD.

The concentrations of urushiol used for sensitization (2.0%) and challenge (0.5%) in the mouse model in the present study are within the range of concentrations known to elicit contact dermatitis in humans. A patch test study observed that challenge with a 1.0% solution resulted in allergic skin responses (erythema to bullae) in 75% of U.S. volunteers, representative of the degree of sensitization estimated to be present in the U.S. population (19). Leaves of the plants belonging to the Toxicodendron family, such as poison ivy, oak, and sumac, contain up to 2.5% urushiol (wt/wt) that is concentrated in resin droplets on the leaf surface (27). The resin of the Japanese lacquer tree, also of the Toxicodendron family and known to cause occupational allergies in lacquer workers, contains between 55% and 75% urushiol (28). Thus, local skin exposures are heterogenous, but well within the range of concentrations used in our study.

Emerging data have demonstrated that certain cytokines and chemokines can act as endogenous itch mediators (29). Some cytokines are released from skin and immune cells and contribute to the cross-talk between the immune and nervous systems. Examples include IL-31 and CXCL10, which were shown to signal through their cognate receptors on primary sensory neurons to induce itch. However, we did not observe up-regulation of IL-31 and CXCL10 transcription in the skin of urushiol-challenged mice, indicating that these cytokines do not contribute to the observed pathology, with IL-33 fulfilling this role instead (Tables S1 and S2). Nevertheless, because we observed residual itch responses in mice after IL-33–/ST2-neutralizing antibody treatment, other endogenous pruritogens or mediators, in addition to IL-33, are likely involved in the itch response of urushiol-induced ACD mice as well and remain to be identified.

IL-33 is a member of the IL-1 cytokine family. In addition to the well-documented role in immune and inflammatory diseases, IL-33/ST2 signaling was also found to contribute to pain (30, 31). Although ST2 expression has been detected in spinal cord neurons and implicated in spinal pain mechanisms, expression and function of ST2 in peripheral sensory neurons have not been explored in detail.

Our study has provided several lines of evidence that suggest functional expression and a physiological signaling role of ST2 in peripheral sensory neurons. First, our qPCR data demonstrate that ST2 transcript is expressed in both mouse and human DRGs. This finding is supported by a recent study that also demonstrated ST2 transcript expression (at a level comparable to the functional IL-5R) in Nav1.8-expressing primary nodose ganglion neurons (32). Second, our immunofluorescence-staining and retrograde-labeling experiments revealed that ST2 is expressed in a subset of small to medium-sized TRPV1-expressing DRG neurons, including neurons that innervate the skin. Immunostaining also identified the presence of ST2 in skin free nerve endings, where IL-33 produced in the skin would have direct access. Thirdly, our Ca^{2+} imaging experiments clearly demonstrated that IL-33 can induce robust Ca^{2+} responses in cultured DRG neurons, and this response is largely abolished by a monoclonal ST2-neutralizing antibody. IL-33 activated Ca^{2+} influx into ∼7% of cultured DRG neurons from naïve mice. Although our immunofluorescence studies detected ST2 in a larger proportion of neurons in sectioned DRGs, the essential binding partner IL-1RAcP was detected in a smaller percentage of cells, suggesting that functional IL-33 receptors, consisting of ST2 and IL-1RAcP, are limited to a relatively small neuronal population. IL-33–induced Ca^{2+} responses in DRG neurons were almost completely abolished in Ca^{2+}-free extracellular solution or by ruthenium red, a TRP channel blocker, and largely abolished by specific TRPA1 and TRPV1 antagonists. It is well established that TRPA1 and TRPV1 are involved in itch transduction (33). Therefore, it is possible that TRPA1 and TRPV1 act downstream of IL-33/ST2 signaling to initiate itch signaling. Lastly, our targeted knockdown of ST2 expression in DRG neurons by i.t. siRNA injection significantly reduced the itch response of urushiol-induced ACD mice. This result further demonstrates the importance of neuronal ST2 in mediating the itch signal under the ACD condition.

Keratinocytes are known as a source of IL-33 in the skin, often induced by proinflammatory factors such as TNF-α and IFN-γ (20). We found that IL-33 expression is significantly increased in the epidermis and is exclusively expressed in keratinocytes under urushiol-induced ACD conditions. The interaction between keratinocytes and primary sensory neurons plays an important role in the development and maintenance of chronic itch conditions (34). Therefore, we propose here that keratinocytes may directly communicate with cutaneous sensory neurons via IL-33, which is released upon tissue inflammation or injury, to promote itch.

The population of IL-33–responsive DRG neurons correlated to a large extent with that of CQ- or histamine-responsive neurons, indicating that IL-33 activates primary sensory neurons that mediate the sensation of itch. In addition, treatment of urushiol-induced ACD mice with IL-33– or ST2-neutralizing antibodies significantly attenuated the scratching response. Cutaneous IL-33 injection rapidly increased scratching behavior in urushiol-challenged mice. IL-33 is known to cause mast cell degranulation and release of histamine (35, 36). However, IL-33–induced itch in the present study is unlikely to be mediated by histamine because the antihistamine, cetirizine, at a dosage that effectively blocks histamine-related itch (37), had no effect on the IL-33–induced itch response. Therefore, these results suggest that IL-33/ST2 signaling may likely mediate allergic itch response through direct activation of itch-sensing primary sensory neurons.

Although our data strongly support a neuronal mechanism of ST2 in mediating itch signaling in urushiol ACD, we cannot rule out the possible participation of more indirect pathways involving nonneuronal cells. It is known that ST2 is expressed in Th2 cells, in a variety of innate immune cells as well as in skin cells (23). IL-33 can interact with keratinocytes, mast cells, and other immune cells through ST2 to produce proinflammatory mediators and cytokines, including TSLP, histamine, serotonin, and IL-13, that have known roles in the initiation of allergic diseases and itch (35, 38–40). Our in vivo experiments using ST2-neutralizing antibodies may have interfered with the actions of these cells types in addition to the sensory neurons. These cells may also contribute to the residual scratching behavior we observed

in mice injected with ST2-neutralizing antibodies, and the pathways involved remain to be studied.

Our study showed that IL-33 did not elicit any obvious scratching behavior in naïve mice, but did evoke significantly more itch-related scratching after urushiol challenge. In line with this finding, we observed that IL-33–induced Ca^{2+} responses are more pronounced in DRG neurons from urushiol-treated mice than from naïve mice. The above phenomenon is likely due to the sensitization of itch-signaling pathways under chronic itch conditions. Sensitization of itch-signaling pathways has been proposed as a critical mechanism underlying chronic itch (41, 42). In ACD and atopic dermatitis, nerve fiber densities are increased in the epidermis (43, 44). Extension of these nerve fibers into the epidermis may contribute to spontaneous itch, aggravating itch responses and sensitization of itch signaling pathways (42). Enhanced animal behavioral scratching and DRG neuron responses to pruritogens have been documented in a mouse chronic dry-skin model (45). Similarly, CXCL10, which is a nonpruritogenic chemokine in naïve mice, was found to turn into a potent pruritogen in the inflamed skin of a mouse model of ACD (14). Along the same lines, it is likely that urushiol-induced ACD sensitizes itch-signaling pathways, such that IL-33 becomes a pruritogen to evoke itch responses under the ACD condition.

Our findings suggest that blocking IL-33/ST2 signaling may represent a therapeutic approach to ameliorate itch and skin inflammation in poison ivy ACD and, possibly, other chronic itch conditions in which IL-33/ST2 signaling may participate. Currently, ACD patients are treated with antihistamines and corticosteroids. Antihistamines are largely ineffective to counteract itch, an observation replicated in our mouse model in which cetirizine failed to suppress the scratching behavior. Corticosteroids have known side effects and need to be administered early after exposure to be effective. Therapies targeting IL-33/ST2 signaling may be especially useful in individuals known to develop severe anaphylactic complications after allergen exposure and in individuals known to develop life-threatening respiratory allergic responses to urushiol, including forest firefighters for whom poison ivy is an occupational hazard (4).

Materials and Methods

Animals. Experimental procedures were approved by the Institutional Animal Care and Use Committee of Duke University. Male C57BL/6 mice (6–8 wk old) were purchased from The Jackson Laboratory. Mice were housed at facilities accredited by the Association for Assessment and Accreditation of Laboratory Animal Care in standard environmental conditions (12-h light–dark cycle and 23 °C). Food and water were provided ad libitum.

Urushiol/Oxazolone-Induced Allergic Contact Dermatitis Model. C57BL/6 male mice were sensitized by applying 2.0% (wt/vol) urushiol or oxazolone to the shaved abdomen. After 5 d (day 0), mice were challenged with 0.5% urushiol or oxazolone by painting on the shaved nape of the neck. On days 2 and 4, mice were challenged with urushiol or oxazolone in the same way as day 0, for a total of three to five challenges.

Scratching Behavior Analysis. Behavioral experiments were performed as described (16). All behavioral tests were performed by an experimenter blinded to experimental conditions.

DRG Neuron Culture and Ca^{2+} Imaging. C1-T1 bilateral mouse DRGs from either acetone- or urushiol-treated mice were dissociated as described (46). Ca^{2+} imaging using Fura-2 was performed 24 h after DRG dissection.

Mouse Transcriptome Microarray. RNA samples were processed by Affymetrix GeneChip Mouse Transcriptome Assay 1.0. The Affymetrix Mouse Transcriptome 1.0 CEL files were imported into Affymetrix Expression Console Software and analyzed by using the Gene Level-SST RMA normalization method. The datasets of the microarray analysis are illustrated in Tables S1 and S2.

Retrograde Labeling of Skin-Innervating DRG Neurons. The 0.5% Fast Blue was injected (i.d., 3 μL per site) at seven sites on the shaved nape of the neck of mice under anesthesia. At 4–5 d later, bilateral cervical DRG neurons (C1-T1) were collected.

Immunofluorescent Staining. Immunofluorescent staining was performed and analyzed as described (16).

siRNA Knockdown. Selective ST2 siRNA and scrambled ST2 control siRNA were synthesized by Dharmacon. siRNA was dissolved in 5% glucose and mixed with the in vivo transfection reagent in vivo-jetPEI (Polyplus) and incubated at room temperature for 15 min according to the manufacturer's protocol. Intrathecal injection was performed by a lumbar puncture to deliver reagents to the cerebral spinal fluid under anesthesia. A total of 3 μg of siRNA in 10-μL volume was injected i.t. once a day for two days to knockdown ST2 expression. Two days after the last siRNA injection, C1-T1 DRG neurons and spinal cord tissue were collected and subjected to qPCR or immunostaining to test the efficiency of ST2 knockdown.

Statistics. Statistical analysis were made between groups by using Student's *t* test (for comparison between two groups) or one- or two-way ANOVA (for comparison among three or more groups) followed by Tukey post hoc test. Comparison was considered significantly different if P was <0.05. Data in bar graphs are expressed as means ± SE.

Details of methods and materials are described in *SI Materials and Methods*.

ACKNOWLEDGMENTS. This work was supported by Duke Anesthesiology Dream Innovation Grant 2015-DIG LIU, National Center for Advancing Translational Sciences of the National Institutes of Health Grant UL1 TR001117, Zhejiang Chinese Medical University Start-Up Funding Grant 722223A08301/001/004, and National Nature Science Foundation of China Grant 81603676 (to B.L.); and National Institute of Environmental Health Sciences Grants R01 ES015056 and U01 ES015674 and National Institute of Arthritis and Musculoskeletal and Skin Disease Grant R21 AR070554 (to S.-E.J.).

1. Kaplan DH, Igyártó BZ, Gaspari AA (2012) Early immune events in the induction of allergic contact dermatitis. *Nat Rev Immunol* 12(2):114–124.
2. Boelman DJ (2010) Emergency: Treating poison ivy, oak, and sumac. *Am J Nurs* 110(6):49–52.
3. Gladman AC (2006) Toxicodendron dermatitis: Poison ivy, oak, and sumac. *Wilderness Environ Med* 17(2):120–128.
4. Epstein WL (1994) Occupational poison ivy and oak dermatitis. *Dermatol Clin* 12(3):511–516.
5. Lee NP, Arriola ER (1999) Poison ivy, oak, and sumac dermatitis. *West J Med* 171(5-6):354–355.
6. Sasseville D (2009) Clinical patterns of phytodermatitis. *Dermatol Clin* 27(3):299–308, vi.
7. Mohan JE, et al. (2006) Biomass and toxicity responses of poison ivy (*Toxicodendron radicans*) to elevated atmospheric CO2. *Proc Natl Acad Sci USA* 103(24):9086–9089.
8. Ziska LH, Epstein PR, Schlesinger WH (2009) Rising CO(2), climate change, and public health: Exploring the links to plant biology. *Environ Health Perspect* 117(2):155–158.
9. Canavan D, Yarnell E (2005) Successful treatment of poison oak dermatitis treated with *Grindelia* spp. (gumweed). *J Altern Complement Med* 11(4):709–710.
10. Colbeck C, Clayton TH, Goenka A (2013) Poison ivy dermatitis. *Arch Dis Child* 98(12):1022.
11. Usatine RP, Riojas M (2010) Diagnosis and management of contact dermatitis. *Am Fam Physician* 82(3):249–255.
12. LaMotte RH, Dong X, Ringkamp M (2014) Sensory neurons and circuits mediating itch. *Nat Rev Neurosci* 15(1):19–31.
13. Cevikbas F, et al. (2014) A sensory neuron-expressed IL-31 receptor mediates T helper cell-dependent itch: Involvement of TRPV1 and TRPA1. *J Allergy Clin Immunol* 133(2):448–460.
14. Qu L, Fu K, Yang J, Shimada SG, LaMotte RH (2015) CXCR3 chemokine receptor signaling mediates itch in experimental allergic contact dermatitis. *Pain* 156(9):1737–1746.
15. Wilson SR, et al. (2013) The epithelial cell-derived atopic dermatitis cytokine TSLP activates neurons to induce itch. *Cell* 155(2):285–295.
16. Liu B, et al. (2013) TRPA1 controls inflammation and pruritogen responses in allergic contact dermatitis. *FASEB J* 27(9):3549–3563.
17. Liu Q, et al. (2009) Sensory neuron-specific GPCR Mrgprs are itch receptors mediating chloroquine-induced pruritus. *Cell* 139(7):1353–1365.
18. Zhao ZQ, et al. (2013) Chronic itch development in sensory neurons requires BRAF signaling pathways. *J Clin Invest* 123(11):4769–4780.
19. Epstein WL, Baer H, Dawson CR, Khurana RG (1974) Poison oak hyposensitization. Evaluation of purified urushiol. *Arch Dermatol* 109(3):356–360.
20. Taniguchi K, et al. (2013) Interleukin 33 is induced by tumor necrosis factor alpha and interferon gamma in keratinocytes and contributes to allergic contact dermatitis. *J Investig Allergol Clin Immunol* 23(6):428–434.
21. Mattii M, et al. (2013) The balance between pro- and anti-inflammatory cytokines is crucial in human allergic contact dermatitis pathogenesis: The role of IL-1 family members. *Exp Dermatol* 22(12):813–819.
22. Imai Y, et al. (2013) Skin-specific expression of IL-33 activates group 2 innate lymphoid cells and elicits atopic dermatitis-like inflammation in mice. *Proc Natl Acad Sci USA* 110(34):13921–13926.

23. Molofsky AB, Savage AK, Locksley RM (2015) Interleukin-33 in tissue homeostasis, injury, and inflammation. *Immunity* 42(6):1005–1019.
24. Shimada SG, LaMotte RH (2008) Behavioral differentiation between itch and pain in mouse. *Pain* 139(3):681–687.
25. De Jong WH, et al. (2009) Contact and respiratory sensitizers can be identified by cytokine profiles following inhalation exposure. *Toxicology* 261(3):103–111.
26. Dhingra N, et al. (2014) Molecular profiling of contact dermatitis skin identifies allergen-dependent differences in immune response. *J Allergy Clin Immunol* 134(2):362–372.
27. Gartner B, Wasser C, Rodriguez E, Epstein W (1993) Seasonal variation of urushiol content in poison oak leaves. *Am J Contact Dermat* 4(1):33–36.
28. Yukio K, Tetsuo M (2001) Synthesis of urushiol components and analysis of urushi sap from *Rhus vernicifera*. *J Oleo Sci* 50:865–874.
29. Storan ER, O'Gorman SM, McDonald ID, Steinhoff M (2015) Role of cytokines and chemokines in itch. *Handbook Exp Pharmacol* 226:163–176.
30. Zarpelon AC, et al. (2016) Spinal cord oligodendrocyte-derived alarmin IL-33 mediates neuropathic pain. *FASEB J* 30(1):54–65.
31. Verri WA, Jr, et al. (2008) IL-33 mediates antigen-induced cutaneous and articular hypernociception in mice. *Proc Natl Acad Sci USA* 105(7):2723–2728.
32. Talbot S, et al. (2015) Silencing nociceptor neurons reduces allergic airway inflammation. *Neuron* 87(2):341–354.
33. Wilson SR, Bautista DM (2014) Role of transient receptor potential channels in acute and chronic itch. *Itch: Mechanisms and Treatment*, Frontiers in Neuroscience, eds Carstens E, Akiyama T (CRC, Boca Raton, FL).
34. Schwendinger-Schreck J, Wilson SR, Bautista DM (2015) Interactions between keratinocytes and somatosensory neurons in itch. *Handbook Exp Pharmacol* 226:177–190.
35. Komai-Koma M, et al. (2012) Interleukin-33 amplifies IgE synthesis and triggers mast cell degranulation via interleukin-4 in naïve mice. *Allergy* 67(9):1118–1126.
36. Haenuki Y, et al. (2012) A critical role of IL-33 in experimental allergic rhinitis. *J Allergy Clin Immunol* 130(1):184–194.e111.
37. Zhu Y, et al. (2009) Participation of proteinase-activated receptor-2 in passive cutaneous anaphylaxis-induced scratching behavior and the inhibitory effect of tacrolimus. *Biol Pharm Bull* 32(7):1173–1176.
38. Ryu WI, et al. (2015) IL-33 induces Egr-1-dependent TSLP expression via the MAPK pathways in human keratinocytes. *Exp Dermatol* 24(11):857–863.
39. Sjöberg LC, Gregory JA, Dahlén SE, Nilsson GP, Adner M (2015) Interleukin-33 exacerbates allergic bronchoconstriction in the mice via activation of mast cells. *Allergy* 70(5):514–521.
40. Kaur D, et al. (2015) IL-33 drives airway hyper-responsiveness through IL-13-mediated mast cell: Airway smooth muscle crosstalk. *Allergy* 70(5):556–567.
41. Han L, Dong X (2014) Itch mechanisms and circuits. *Annu Rev Biophys* 43:331–355.
42. Schmelz M (2014) Sensitization for itch. *Itch: Mechanisms and Treatment*, Frontiers in Neuroscience, eds Carstens E, Akiyama T (CRC, Boca Raton, FL).
43. Kinkelin I, Mötzing S, Koltenzenburg M, Bröcker EB (2000) Increase in NGF content and nerve fiber sprouting in human allergic contact eczema. *Cell Tissue Res* 302(1): 31–37.
44. Fujii M, Akita K, Mizutani N, Nabe T, Kohno S (2007) Development of numerous nerve fibers in the epidermis of hairless mice with atopic dermatitis-like pruritic skin inflammation. *J Pharmacol Sci* 104(3):243–251.
45. Akiyama T, Carstens MI, Carstens E (2010) Enhanced scratching evoked by PAR-2 agonist and 5-HT but not histamine in a mouse model of chronic dry skin itch. *Pain* 151(2):378–383.
46. Liu B, et al. (2013) TRPM8 is the principal mediator of menthol-induced analgesia of acute and inflammatory pain. *Pain* 154(10):2169–2177.

Supporting Information

Liu et al. 10.1073/pnas.1606608113

SI Materials and Methods

Chemicals. Oxazolone was from VWR/Alfa Aesar (catalog no. L00194). Urushiol (15:1) was from Phytolab (catalog no. 81080). HC-030031 was custom-synthesized by Medchem101. AMG9810 was from Tocris. Cap, MO, CQ, and histamine were from Sigma-Aldrich.

Urushiol/Oxazolone-Induced Allergic Contact Dermatitis Model. Mice were sensitized by applying 2.0% (wt/vol) urushiol or oxazolone (dissolved in a 4:1 mixture of acetone:olive oil; volume of 30 μL) to the shaved abdomen under anesthesia by ketamine/xylazine. After 5 d (day 0), mice were challenged with 0.5% urushiol or oxazolone dissolved in acetone (40 μL) by painting on the shaved nape of the neck. On days 2 and 4, mice were challenged with urushiol or oxazolone in the same way as day 0, for a total of three to five challenges.

Scratching Behavior Analysis. Mice were placed in the observation chamber to acclimate for 40 min. Then, mice were videotaped at time points of 0 and 4 h (in some cases after 24 h) after urushiol challenge. A series of one or more scratching movements by the hind paw directed toward the neck area was defined as a scratching bout, which ended when the mouse either licked its hind paw or placed its hind paw back on the floor. The total number of scratching bouts was counted for 30 min. In cases where the mouse cheek model was used, the mouse right cheek was shaved before, and the scratching using the hind paw and wiping using the forepaw toward the cheek area was counted for 30 min. All behavioral tests were performed by an experimenter blinded to experimental conditions.

Drug Administration. For blocking IL-33 and ST2 signaling, mouse IL-33–neutralizing and ST2-neutralizing antibodies (catalog nos. AF3626 and MAB10041; R&D Systems) and normal goat or rat isotype control IgGs (catalog nos. I5256 and I4131; Sigma-Aldrich) were dissolved in sterile PBS. Mice were given neutralizing antibodies i.p. daily 30 min before each urushiol challenge for a total of five times. For control groups, urushiol-challenged mice were given the same amount of isotype IgGs.

For IL-33–injection experiments, IL-33 (R&D Systems) was prepared in PBS plus 0.1% BSA. IL-33 was injected into the nape of neck (300 ng per site, 20-μL injection volume, i.d.). Control group mice received the same amount of PBS + 0.1% BSA injection. In cases where ST2-neutralizing antibody was coapplied with IL-33, ST2 antibody (50 μg per site) was mixed with IL-33 and injected into the nape of the neck as mentioned above.

Bifold Skin Thickness and Dermatitis Evaluation. The increase in bifold skin thickness was measured by using a digital spring-loaded thickness gauge (Mitutoyo Quick Mini 700-118-20) and was calculated by subtracting the values before sensitization from those obtained from specific days afterward. Six determinations were made at different dorsal skin sites per mouse and averaged. The severity of dermatitis was scored following described criteria (48) as follows: Individual scores (0, none; 1, mild; 2, moderate; 3, severe) of dryness, excoriation, erythema, and swelling were summed up as the dermatitis score by an experimenter blinded to the treatment groups.

DRG Neuron Culture and Ca^{2+} Imaging. C1-T1 bilateral mouse DRGs from either acetone- or urushiol-treated mice were dissociated by using 0.28 Wünsch units/mL Liberase Blendzyme 1 (Roche Diagnostics) as described (26). Ca^{2+} imaging was performed 24 h after DRG dissection. Medium was replaced by modified standard Ringer's bath solution (in mM: 140 NaCl, 5 KCl, 2 $CaCl_2$, 2 $MgCl_2$, 10 Hepes, and 8 glucose, pH 7.4). For Ca^{2+}-free extracellular solution, $CaCl_2$ was substituted by equal molar EGTA. Cells were loaded with Fura-2-AM (10 μM; Invitrogen) for 45 min. Ratiometric Ca^{2+} imaging was performed on an Olympus IX51 microscope with a Polychrome V monochromator (Till Photonics) and a PCO Cooke Sensicam QE CCD camera and Imaging Workbench 6 imaging software (PCO AG).

RNA Extraction, Mouse Transcriptome Microarray, and Data Analysis. At 4 h after the last challenge, mice were euthanized, and neck skins were collected. RNA was extracted by TRIzol RNA isolating reagent (Thermo Fisher Scientific) plus an RNeasy Mini Kit (Qiagen). RNA quality and purity were validated by TapeStation (Agilent) and NanoDrop (Thermo Fisher Scientific) analysis. Only RNA samples showing RNA Integrity Number ≥ 8.0 and A260/230 ≥ 1.5 were used for RNA microarray library construction. For each library construction, 400 ng of total RNAs was used. The samples were then processed by Affymetrix GeneChip Mouse Transcriptome Assay 1.0. The Affymetrix Mouse Transcriptome 1.0 CEL files were imported into Affymetrix Expression Console Software (Version 1.4). The CEL files were analyzed by using the Gene Level-SST RMA normalization method, according to the user manual. The Gene Level-SST RMA files (CHP files) were imported into the Affymetrix Transcriptome Analysis Console (TAC) 3.0 software, according to the user guide, for further analysis. ANOVA analysis was made among the vehicle-, oxazolone-, and urushiol-treated groups. Data were analyzed with help from bioinformatics specialists in the Duke University Core Facility.

Real-Time PCR (qPCR). For qPCR, cDNA synthesis was performed by using a high-capacity RNA-to-cDNA Kit (Applied Biosystems). qPCR was performed with the LightCycler 480 real-time PCR system (Roche). Each sample was run in triplicate. Human or mouse samples were normalized to human GAPDH or mouse Actb, respectively. CT values were determined by using Light-Cycler 480 software and averaged. Relative quantification was determined by the ΔΔCT method. Taqman probes used were as follows: hGAPDH (4332694), hIL1RL1 (Hs00249384_m1), hIL1R3 (00991010_m1), mActb (Mm02619580_g1), mTrpa1 (Mm01227437_m1), mIl1rl1 (Mm00516117_m1), mIl1r3 (Mm00434237_m1), and mIl33 (Mm00505403_m1). Total RNA extracted from adult human DRG (catalog no. 636150) was purchased from Clontech. According to the manufacturer, total RNA source was "Normal human dorsal root ganglion pooled from 21 male/female Caucasians, ages: 16-65; cause of death: sudden death."

Skin Protein Isolation and ELISA. At 4 h after the last oxazolone or urushiol challenge, mice were euthanized, and 4-mm biopsies were excised from the nape of the neck and immediately frozen in liquid nitrogen. Tissue was homogenized by using a Bullet Blender (NextAdvance) in 50 mM Tris base (pH 7.4) and 150 mM NaCl with protease inhibitor and 0.2% Triton X. Homogenization was carried out for 20 min at full speed. Then samples were centrifuged at 10,000 × *g* for 10 min at 4 °C. The supernatant was tested by IL-33 ELISA (R&D Systems).

Retrograde Labeling of Skin-Innervating DRG Neurons. The 0.5% Fast Blue was injected (i.d., 3 μL per site) at seven sites on the shaved nape of the neck of mice under anesthesia. At 4–5 d later,

mice were euthanized, and bilateral cervical DRG neurons (C1-T1) were collected and embedded in OCT for immunohistochemistry.

Immunofluorescent Staining and Analysis. Mouse bilateral C1-T1 DRGs were removed and immersed immediately in 4% paraformaldehyde overnight at 4 °C. Mouse skin from the unchallenged group or oxazolone- or urushiol-challenged group were collected and frozen in frozen tissue matrix (OCT). Mouse DRGs and skins were then cut by cryostat in 8-μm sections (Leica Biosystems). The skin was postfixed with cold acetone for 10 min and air-dried before immunostaining. For immunostaining, the sections were first blocked with 1% BSA plus 10% donkey serum for 2 h at room temperature. The sections were then incubated overnight at 4 °C with the following primary antibodies: ST2 (catalog no. PA-5-23316; Pierce), IL-33 (catalog no. AF3626; R&D Systems), Keratin 14 (catalog no. PA-5-13672; Pierce), PGP9.5 (catalog no. ab10410; Abcam), TRPV1 (catalog no. GT15129; Neuromics), and GS and IL-1RAcP (catalog nos. sc-6640 and sc-47056; Santa Cruz Biotechnology). The sections were then incubated for 1 h at room temperature with corresponding secondary fluorescent antibodies (1:1,000; Invitrogen).

For the determination of the specificity of the ST2 antibody, the antigenic peptide preabsorption/neutralization method was used according to the manufacturer's instructions. A blocking peptide with the antigenic sequence of the ST2 protein (CPRQGKPSYTVDWYYSQT) was synthesized (Thermo Fisher Scientific). The ST2 antibody was mixed with a fivefold (by weight) excess of the blocking peptide in TBS+0.25% Triton X-100. The mixture was then incubated for 2 h at room temperature. Then, the normal staining protocol as described above was followed using the ST2 antibody only or ST2 antibody+blocking peptide. The staining intensities of these two groups were compared thereafter. DRG neurons were identified by Nissl stain, a commonly used method for neuron-specific staining (9, 10). For skin sections, skin cells were identified by counterstain with DAPI (Invitrogen).

Images were obtained with a Zeiss Imager Z1 microscope equipped with ApoTome and analyzed by ZEN software (Zeiss). Quantification of immunofluorescence staining was carried out by an observer blinded to the grouping. The percentage of the staining area in each of selected images was calculated by ImageJ software (NIH). Five images were randomly selected per mouse tissue and then averaged and compared. The immunofluorescence intensity of individual neurons was calculated by using ZEN software (Zeiss).

Statistics. Statistical analysis of differences between groups were performed using Student's *t* test (for comparison between two groups) or one- or two-way ANOVA (for comparison among three or more groups) followed by Tukey post hoc test. Data were considered significantly different at P of < 0.05. Data in bar graphs are expressed as means ± SE.

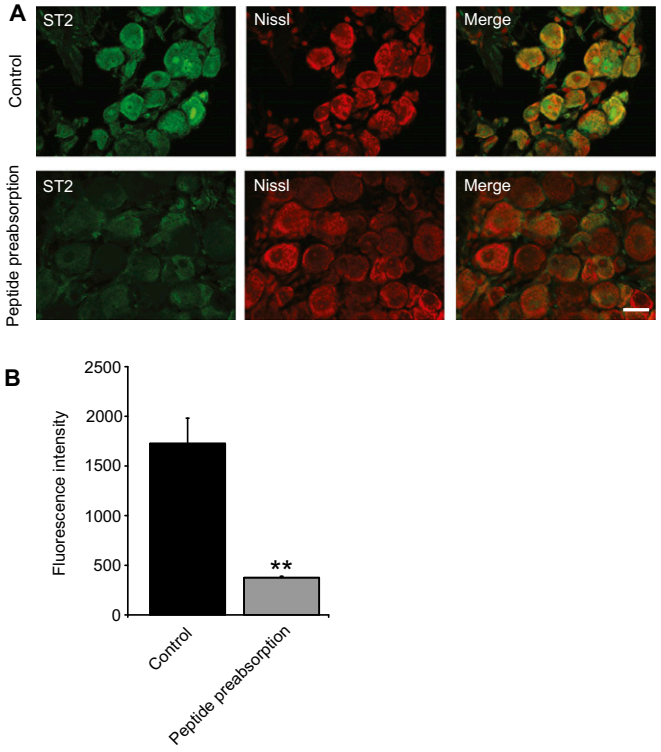

Fig. S1. Antigenic peptide preabsorption blocks ST2 antibody staining. (*A*) Representative immunostaining images of mouse DRG neurons using ST2 antibody alone (Control) or ST2 antibody+blocking peptide (Peptide preabsorption). (*B*) Summary of the fluorescence intensities of neurons stained with ST2 antibody (Control) or ST2 antibody+blocking peptide (Peptide preabsorption). A total of 65 and 68 neurons were included in each group, respectively. (Scale bar, 20 μm.) $^{**}P < 0.01$. Student's *t* test was used for the analysis.

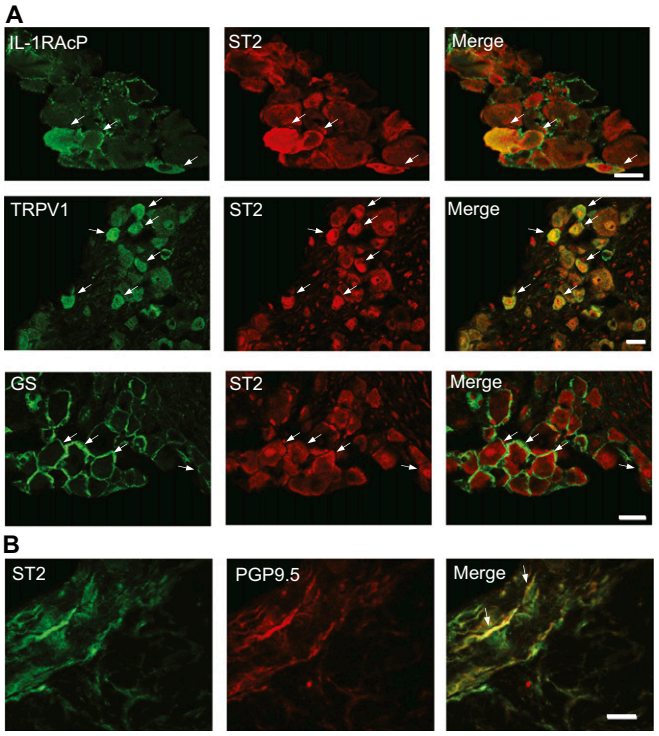

Fig. S2. Characterization of ST2 expression in DRG neurons and skin nerve fibers. (*A*) Immunostaining showing the overlapping of ST2 with the accessory subunit IL-1RAcP and TRPV1 that labels nociceptive sensory DRG neurons but not with GS that labels satellite glial cells. (*B*) Immunostaining showing the overlapping of ST2 with PGP9.5-positive nerve fibers in mouse skin. (Scale bars, 20 μm.)

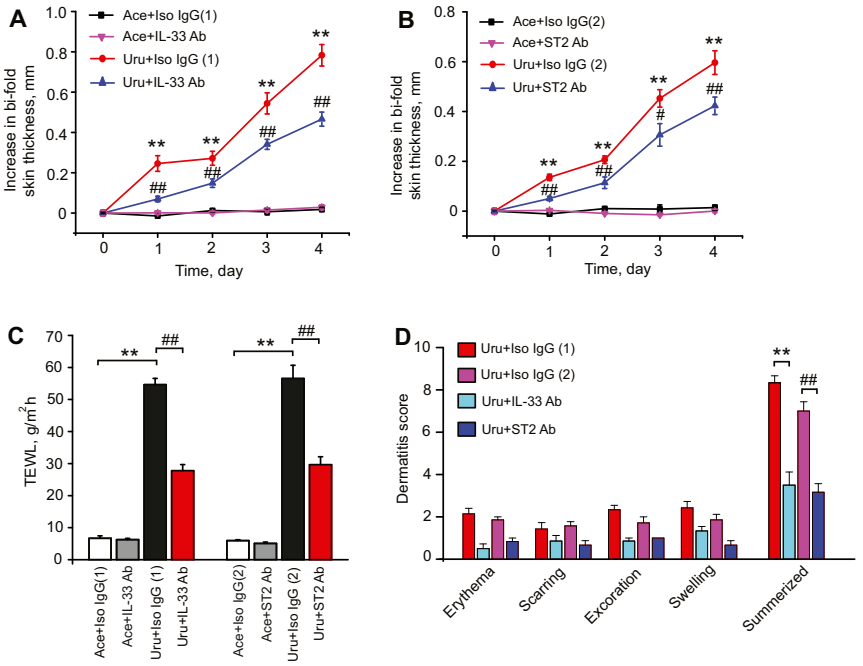

Fig. S3. Effects of inhibition of IL-33/ST2 signaling on skin inflammation of urushiol-challenged mice. (*A* and *B*) Bifold thickness of neck skin measured daily. (*C*) TEWL measured at the neck skin 24 h after the last (fifth) neutralizing antibody or isotype control IgGs treatment. (*D*) Dermatitis score of urushiol-challenged mice treated with isotype control IgGs or IL-33– or ST2-neutralizing antibody. $n = 7$ or 8 mice per group. $^{**}P < 0.01$; $^{\#\#}P < 0.01$. One- or two-way ANOVA followed by Tukey post hoc test was used for statistical analysis.

Table S1. Transcriptome microarray datasets of oxazolone-induced ACD group vs. vehicle group

Table S1

Table S2. Transcriptome microarray datasets of urushiol-induced ACD group vs. vehicle group

Table S2